

Small and Arbitrary Amplitude Dust-Acoustic Solitary Waves with Nonextensive Electrons and Vortex-like Distributed Ions

G. Mandal^{1,*}, A. Paul¹, K. Roy² and M. Asaduzzaman³

¹*Department of Electronics and Communications Engineering,
East West University, Aftabnagar, Dhaka 1212, Bangladesh*

²*Beluti M. K. High School, P.O. Beluti, Dist. Birbhum, West Bengal, India*

³*Institute of Natural Science, United International University,
Dhanmondi, Dhaka-1209, Bangladesh*

* *gdmandal@ewubd.edu*

(Received: 22 September 2016 published: XX March 2017)

Abstract. The modified Korteweg-de Vries (KdV) equation is derived in this study for dust-acoustic (DA) solitary waves in an unmagnetized dusty plasma consisting of q -nonextensive electrons, vortex-like (trapped) distributed ions. The reductive perturbation technique has been employed to derive the modified KdV equation. A non-linear pseudo-potential technique is also employed to investigate arbitrary amplitude DA solitary waves. Numerical results show the variation of amplitude, phase velocity and width of the nonlinear waves for different parameters.

Keywords: Nonextensive electrons; Vortex-like distribution; Dusty plasma; Solitary waves; Dust-acoustic wave.

I. INTRODUCTION

The properties of dust-acoustic (DA) waves are studied vigorously for the last few years to understand the properties of localized electrostatic perturbations in space and laboratory dusty plasmas [1–6]. Shukla and Eliasson [7] have published a model where they described how large amplitude DA waves in dusty plasmas behave. It has been found both theoretically [8] and experimentally [9] that the dynamics of very massive and high charged dust grains introduces new eigenmodes. One of these is the low-frequency DA mode [8, 9], where the dust-particle mass provides the inertia and the pressures of inertia less electrons and ions provide the restoring force [10].

It has been found that electron and ion distribution play an important role in characterizing the physics of nonlinear waves. In the recent past, the nonlinear DA waves have been investigated both theoretically [11–14] as well as experimentally [15, 16] by a large number of authors, taking into

account the equilibrium plasma species that follow the Maxwellian distribution. For the systems with the long-range interactions, such as plasma and gravitational systems involving non-equilibrium stationary states, Maxwellian distribution might be inadequate for the proper description.

It is evident that the high energy tails display strong deviation from simple Maxwellian due to the anisotropy of the temperature and long range interactions caused by the coupling between plasmas and external fields. Such particles, following non-Maxwellian distribution function point to a class of Tsallis velocity distribution [17], are very important to describe the non-equilibrium stationary states such as long-range interactions [18] among the plasma species, global correlations [19] among the self-gravitating systems, long-time memory effects, etc. This type of velocity distribution [17] is known as q -distribution which characterizes the nonextensivity of any plasma species. Nowadays, nonextensive [17] plasma has received deserved attention due to its wide relevance in astrophysical and cosmological scenarios like stellar polytropes [20], hadronic matter and quark-gluon plasma [21], etc. It is important to note that $q = 1$ corresponds to Maxwellian distribution and $q \neq 1$ denotes the q -distribution point to a class of Tsallis velocity distribution [17]. The distribution for $q \neq 1$ follows a power law distribution instead of usual exponential law. The nonextensive parameter q is taken to be constant and very close to the value for which ordinary statistical mechanics is obtained ($q = 1$), meaning that all calculations can be performed in the leading order to $(q-1)$, with no considerable loss of information [22].

Recently, Tribeche and Merriche [23] stressed about nonextensive DA SWs where soliton exhibits compression for $q < 0$ and rarefaction for $q > 0$. Eslami *et al.* [24] have investigated the geometric effects on DIA SWs by assuming electron nonextensivity. Very recently, Yasmin *et al.* [25] proposed three components dust fluid model and discussed the mutual balance of nonlinearity and dissipation taking into account the electron nonextensivity. Large amplitude SWs have also been addressed by Tribeche *et al.* [26] following q -nonextensive electron distribution. Since electron is 1836 times lighter than ion, it can rapidly transfer high energy from one place to another. The suitability of electron nonextensivity has already been proposed and established by several authors [24–26].

Pakzad [27] studied the effect in strongly coupled dusty plasmas containing Boltzmann distributed ions and q -nonextensive electrons. They derived the Korteweg-de Vries-Burgers equation and found that the nonextensive property of the electrons has a quantitative effect on the shock waves potentials. Awady and Djebli [1] studied the different features of DA waves in strongly coupled unmagnetized dusty plasma where both electron and ion follow q -nonextensive distribution and considered negatively charged mobile dust. They have investigated the dependence of the solitary and shock excitation characteristics based on the nonextensive parameter, electron to ion concentration ratio, and ion to electron temperature ratio. Roy *et al.* [28] also studied the shock waves in a dusty plasma having q -nonextensive electron velocity distribution.

In most of the studies of dusty plasma, negatively charged dust grains have been considered in addition to electrons and ions as the plasma species [29–31]. Amin *et al.* [32] studied DA waves in an unmagnetized three-component dusty plasma consisting of mobile charge fluctuating positive dust, trapped electrons and Boltzmann-distributed ions. They have found that the properties of DA solitary waves are modified when dust charge fluctuation and trapped electrons are considered. Alinejad [33] has shown that the trapped electrons introduce a strong nonlinearity and that the

trapped electrons can support solitary waves with only compressive structures. No scientific phenomena can still be established where ions can be trapped and electron is nonextensive.

In this paper, we consider the nonlinear propagation of DA waves in an unmagnetized dusty plasma environment with q -nonextensive electrons and vortex-like distributed (trapped) ions. Standard reductive perturbation technique [34] has been used to derive the modified Korteweg-de Vries (KdV) equation. Some authors [35–38] studied DA solitons of large amplitude using the Sagdeev's pseudo-potential analysis [38]. Motivated by this, we also discuss the effect of nonextensive electron on arbitrary amplitude DA solitary structures using pseudo-potential approach.

II. GOVERNING EQUATIONS

We consider a 1-D, three component unmagnetized dusty plasma consisting of q -nonextensive electrons, vortex-like distributed ions and mobile negative dust. The equilibrium state of the dusty plasma system under this condition is defined as $n_{e0} + z_d n_{d0} = n_{i0}$, where n_{e0} , n_{i0} and n_{d0} are the equilibrium number density of electron, ion and dust, respectively, and z_d is the charge state of dust.

The dynamics of the DA waves in such a dusty plasma system is described by the following set of equations:

$$\frac{\partial n_d}{\partial t} + \frac{\partial}{\partial x}(n_d u_d) = 0, \quad (1)$$

$$\frac{\partial u_d}{\partial t} + u_d \frac{\partial u_d}{\partial x} = \left(\frac{z_d e}{m_d} \right) \frac{\partial \phi}{\partial x}, \quad (2)$$

$$\frac{\partial^2 \phi}{\partial x^2} = 4\pi e(n_e - n_i + z_d n_d), \quad (3)$$

where n_d is the dust number density, u_d is the dust fluid speed, m_d is dust mass, ϕ is the electrostatic wave potential, n_e is the electron number density, n_i is the ion number density.

As we consider the q -nonextensive distributed ions, so we can express n_e and n_i respectively as:

$$n_e = n_{e0} \left[1 - (q-1) \frac{e\phi}{kT_e} \right]^{\frac{1}{q-1}}, \quad (4)$$

$$n_i = n_{i0} \left[1 - \frac{e\phi}{kT_i} - \frac{4}{3\sqrt{\pi}} (1-\delta) \left(-\frac{e\phi}{kT_i} \right)^{3/2} + \frac{1}{2} \frac{e^2 \phi^2}{k^2 T_i^2} \right], \quad (5)$$

where q is a real number and $q > -1$, δ is a parameter that determines the number of trapped ions, whose magnitude is defined by the ratio of free ion temperature and trapped ion temperature, T_e and T_i are respectively the electron and ion temperatures. The electron distribution has already been discussed by several authors [23, 25, 26]. The vortex-like ion is also found by several authors [39–41].

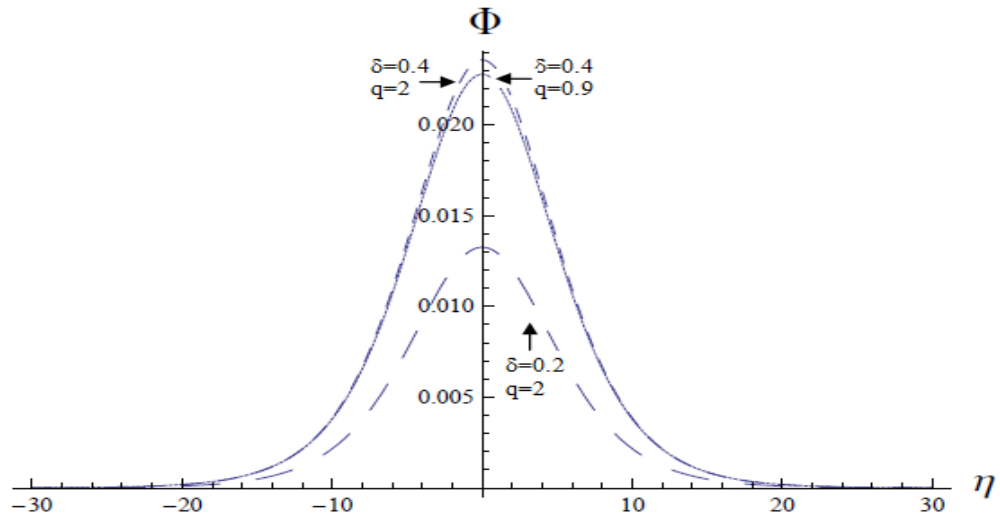


FIGURE 1. The variation of the solution Φ of the modified KdV equations with η for $T_e = 1.3 \times 10^{-11}$ erg , $T_i = 4.8 \times 10^{-13}$ erg , $\delta = 0.4$ and $q = 0.9$ (solid curve), $\delta = 0.4$ and $q = 2$ (dotted curve), $\delta = 0.2$ and $q = 2$ (long-dashed curve).

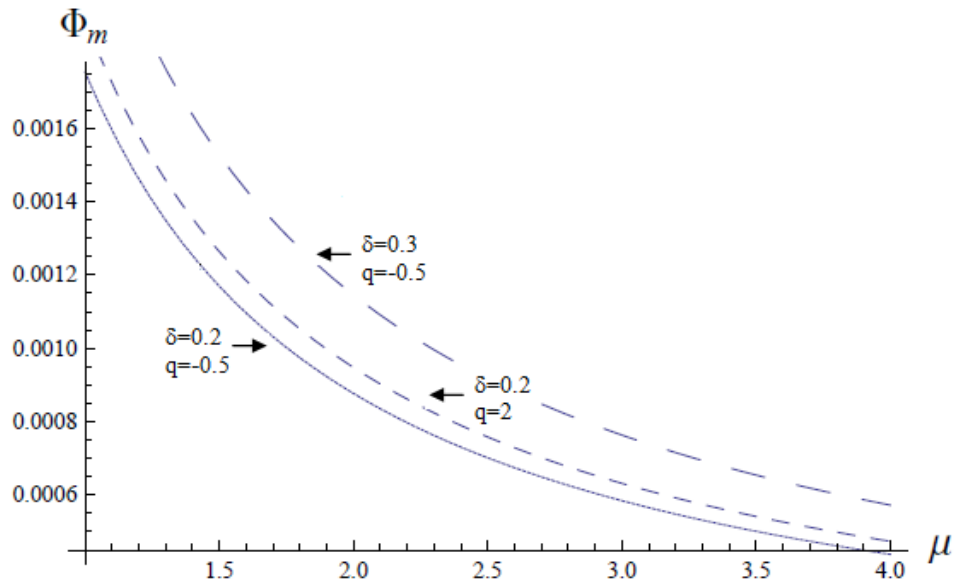


FIGURE 2. The variation of the amplitude Φ_m with μ for $\delta = 0.2$ and $q = -0.5$ (solid curve), $\delta = 0.2$ and $q = 2$ (dotted curve), $\delta = 0.3$ and $q = -0.5$ (long-dashed curve).

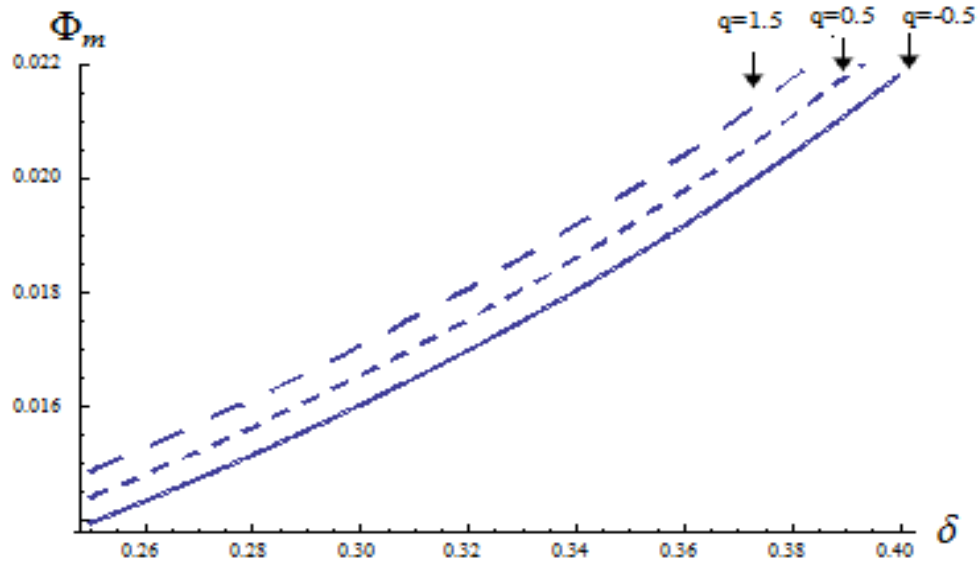


FIGURE 3. The variation of the amplitude Φ_m with δ for $q = -0.5$ (solid curve), $q = 0.5$ (dotted curve) and $q = 1.5$ (long-dashed curve).

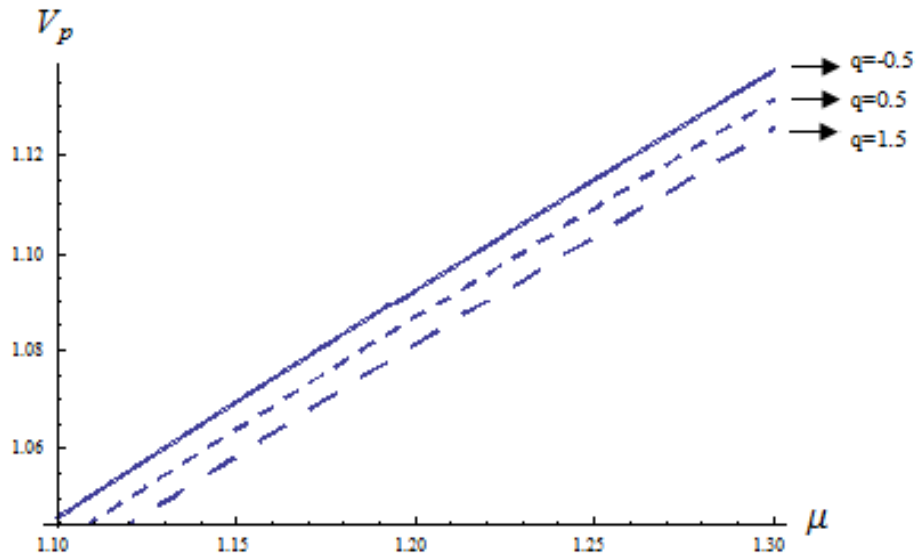


FIGURE 4. The variation of the wave phase velocity V_p with μ for $q = -0.5$ (solid curve), $q = 0.5$ (dotted curve) and $q = 1.5$ (long-dashed curve).

We consider the normalized variables: $N = n_d / n_{d0}$, $X = x / \lambda_D$, $U = u_d / C_d$, $\Phi = e\phi / kT_i$ and $T = t\omega_{pd}$, $\lambda_D = (kT_i / 4\pi z_d e^2 n_{d0})^{1/2}$, $C_d = (z_d kT_i / m_d)^{1/2}$ and $\omega_{pd} = (4\pi z_d^2 e^2 n_{d0} / m_d)^{1/2}$. The normalized form of equations (1)- (3) are given below:

$$\frac{\partial N}{\partial T} + \frac{\partial}{\partial X}(NU) = 0, \quad (6)$$

$$\frac{\partial U}{\partial T} + U \frac{\partial U}{\partial X} = \frac{\partial \Phi}{\partial X}, \quad (7)$$

$$\begin{aligned} \frac{\partial^2 \Phi}{\partial X^2} = \frac{1}{\mu} & \left[\gamma \left(1 + \frac{q+1}{2} \sigma \Phi + \frac{(q+1)(3-q)}{8} \sigma^2 \Phi^2 + \frac{(q+1)(3-q)(5-3q)}{48} \sigma^3 \Phi^3 + \dots \right) \right] \\ & - \frac{1}{\mu} \left[\left(1 - \Phi - \frac{4}{3\sqrt{\pi}} (1-\delta)(-\Phi)^{3/2} + \frac{1}{2} \Phi^2 \right) - \mu N \right], \end{aligned} \quad (8)$$

where $\sigma = T_i / T_e$, $\mu = z_d n_{d0} / n_{i0}$ and $\gamma = n_{e0} / n_{i0}$. It would be noted that if the effect of nonextensive electron is absent in equation (8) then the equation is valid for a simple Maxwellian model and the equation reduces to

$$\frac{\partial^2 \Phi}{\partial X^2} = \frac{1}{\mu} \left[\gamma \left(1 + \sigma \Phi + \frac{1}{2} \sigma^2 \Phi^2 + \frac{1}{6} \sigma^3 \Phi^3 + \dots \right) - \left(1 - \Phi - \frac{4}{3\sqrt{\pi}} (1-\delta)(-\Phi)^{3/2} + \frac{1}{2} \Phi^2 \right) + \mu N \right].$$

It is important to note that addition of electron nonextensivity causes the increase of the factor γ , thereafter robustly said that the ion density can be minimized. This is happened due to the trapping of ion following vortex-like distribution. On the other hand, the electron captures high energy, forming high energy tail. The high energy tail displays strong deviation from simple Maxwellian due to the anisotropy of the temperature and long range interactions caused by the coupling between plasmas and external fields.

III. REDUCTIVE PERTURBATION TECHNIQUE (SOLITARY SOLUTION OF MODIFIED KdV EQUATION AND DISCUSSIONS)

To derive the modified KdV equation by employing the reductive perturbation technique [34], we introduce the stretched coordinates [42, 43]:

$$\xi = \varepsilon^{1/4} (X - V_p T), \quad (9)$$

and

$$\tau = \varepsilon^{3/4} T, \quad (10)$$

where ε is a smallness parameter ($0 < \varepsilon < 1$) that measures the weakness of the dispersion, and V_p is the nonlinear wave phase velocity normalized by C_d . Now we expand the variables N , U and Φ in the power series of ε :

$$N = 1 + \varepsilon N^{(1)} + \varepsilon^{3/2} N^{(2)} + \dots, \quad (11)$$

$$U = \varepsilon U^{(1)} + \varepsilon^{3/2} U^{(2)} + \dots, \quad (12)$$

$$\Phi = \varepsilon \Phi^{(1)} + \varepsilon^{3/2} \Phi^{(2)} + \dots, \quad (13)$$

Now substituting these expressions in equations (6)-(8), we get equations of different powers of ε . Solving for $N^{(1)}$, $U^{(1)}$ and V_p we get the following set of relations:

$$N^{(1)} = A_1 \Phi^{(1)}, \quad (14)$$

$$U^{(1)} = -\frac{1}{V_p} \Phi^{(1)}, \quad (15)$$

$$V_p = \sqrt{-\frac{1}{A_1}}, \quad (16)$$

where $A_1 = -[1 + \gamma\sigma(q+1)/2]/\mu$.

Again using equations (11)-(16) and with the help of normalized continuity equation, momentum equation and Poisson's equation we finally derived the following equation:

$$\frac{\partial \Phi^{(1)}}{\partial \tau} + A \sqrt{\Phi^{(1)}} \frac{\partial \Phi^{(1)}}{\partial \xi} + B \frac{\partial^3 \Phi^{(1)}}{\partial \xi^3} = 0 \quad (17)$$

where $A = A_6 / A_5$, $B = 1 / A_5$, $A_2 = 1 - \gamma(q+1)(3-q)\sigma^2 / 4$, $A_3 = \gamma(q+1)(3-q)(5-3q)\sigma^3 / 24$, $A_4 = -3A_1\sqrt{A_3} / 2\sqrt{A_2} - 2(1-\delta)(-1)^{3/2} / \mu\sqrt{\pi}$, $A_5 = 1/V_p^3 - A_1/V_p$, and $A_6 = 3\sqrt{A_3} / 2V_p^2\sqrt{A_2} - A_4$.

Equation (17) is the modified KdV equation. The impact of nonextensive electrons is clearly observable from equation (17). The nonlinear coefficients A and B characterize the nature of the solitary waves. The term nonextensive electrons play a significant role. If nonextensive parameter $q = 1$ then the co-efficient A_2 reduces to Maxwellian distribution. It can be inferred that $q = 1$ causes the maximum nonlinearity [in case of magnitude]. Leading to no loss of energy, the nonlinear co-efficient has less valued if q impinges $< or > 1$. This phenomenal impact is shown in Figure 1. If the magnitude of q is higher or lower than the solitary peak is distinguished lower. Similarly, the nonlinear co-efficient A_3 reduces to one-third of the nonextensive effect if $q = 1$. On the other hand, $q < or > 1$ causes small perturbations. Obviously, nonextensive effects modified the equation.

We can find the steady-state solution of the modified KdV equation by transforming the independent variables ξ and τ to $\eta = \xi - U_0\tau$ and $\tau = \tau$, where U_0 is a constant velocity normalized by C_d , and by imposing appropriate boundary conditions, namely $\Phi \rightarrow 0$, $d\Phi^{(1)} / d\eta \rightarrow 0$, $d^2\Phi^{(1)} / d\eta^2 \rightarrow 0$ as $\eta \rightarrow \pm\infty$. Thus the steady-state solution of the modified KdV equation (17) can be expressed as

$$\Phi^{(1)} = \Phi_m \operatorname{sech}^2 \left(\frac{\xi - U_0\tau}{\Delta} \right), \quad (18)$$

where the amplitude $\Phi_m = (15U_0 / 8A)^2$, and the width $\Delta = \sqrt{16B / U_0}$ (normalized by λ_D).

Now we study the solution (18) of the DA wave for different dusty plasma parameters. In this investigation we have numerically analyzed the wave amplitude Φ_m , the width of the wave Δ , and the wave potential $\Phi = \Phi^{(1)}$ by considering the following set of parameters from the experimental results of Bandyopadhyay *et al.* [16]:

$$n_{i0} = 7 \times 10^7 \text{ cm}^{-3}, \quad n_{e0} = 4 \times 10^7 \text{ cm}^{-3}, \quad n_{d0} = 10^4 \text{ cm}^{-3}, \quad z_d = 10^3, \quad m_d = 10^{-10} \text{ g}, \quad e = 4.8 \times 10^{-10} \text{ CGS unit}, \\ T_e = 1.3 \times 10^{-11} \text{ erg}, \quad T_i = 4.8 \times 10^{-13} \text{ erg}, \quad U_0 = 0.1, \quad \delta = 0.25 - 0.4 \text{ and } q > -1.$$

Figures 1-5 display the results of our investigations from RPT.

Figure 1 shows the variation of the solution $\Phi^{(1)}$ as a function of the parameter η . The solid curve is for $\delta = 0.4$ and $q = 0.9$, the dotted curve is for $\delta = 0.4$ and $q = 2$ and the long-dashed curve is for $\delta = 0.2$ and $q = 2$. From the figure we can conclude that if the number of trapped ions is increased then the potential of the solitary wave increases, but if the nonextensive parameter q increases then the potential of the solitary wave decreases.

Figure 2 is plotted for Φ_m against μ . The solid curve is for $\delta = 0.2$ and $q = -0.5$, the dotted curve is for $\delta = 0.2$ and $q = 2$ and the long-dashed curve is for $\delta = 0.3$ and $q = -0.5$. We observe that the amplitude of the solitary wave decreases with the increment of the parameter μ . Also we found that if we increase either δ or q then the amplitude increases and δ has much more effect on the amplitude compared with q .

Figure 3 displays the variation of Φ_m with δ . The solid curve, the dotted curve and the long-dashed curve are for $q = -0.5$, $q = 0.5$ and $q = 1.5$, respectively. It is clear that the amplitude of the solitary wave increases with the increment of the number of trapped ion. Also higher values of q give higher amplitude.

Figure 4 shows the variation of the phase velocity V_p as a function of the parameter μ . The solid curve, the dotted curve and the long-dashed curve are for $q = -0.5$, $q = 0.5$ and $q = 1.5$, respectively. Phase velocity of the wave increases with the increment of μ , but it decreases with the increment of q .

Figure 5 displays the variation of the width, Δ , of the solitary wave as a function of the parameter μ . The solid curve, the dotted curve and the long-dashed curve are for $q = -0.5$, $q = 0.5$ and $q = 1.5$, respectively. It is found that the width of the wave increases with the increment of μ but decreases with q .

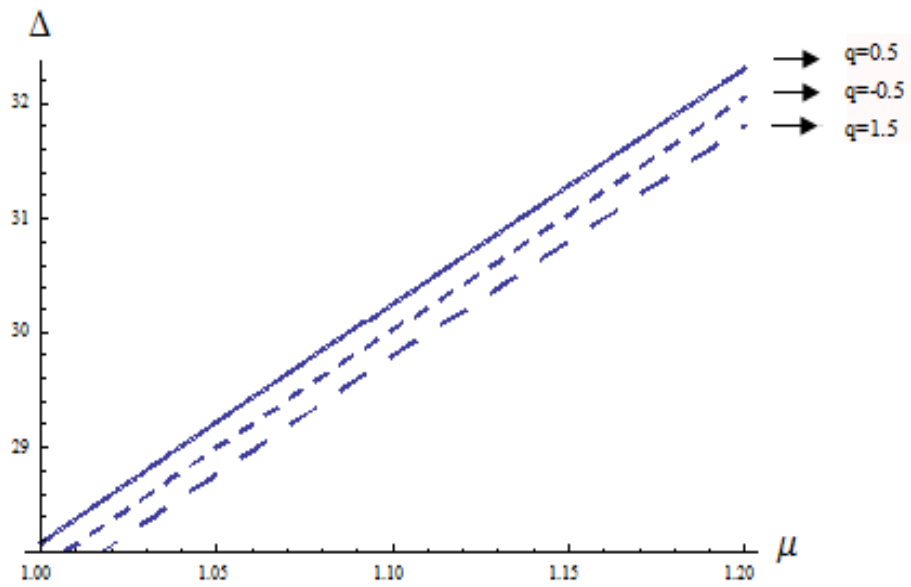


FIGURE 5. The variation of the wave width Δ with μ for $q = -0.5$ (solid curve), $q = 0.5$ (dotted curve) and $q = 1.5$ (long-dashed curve).

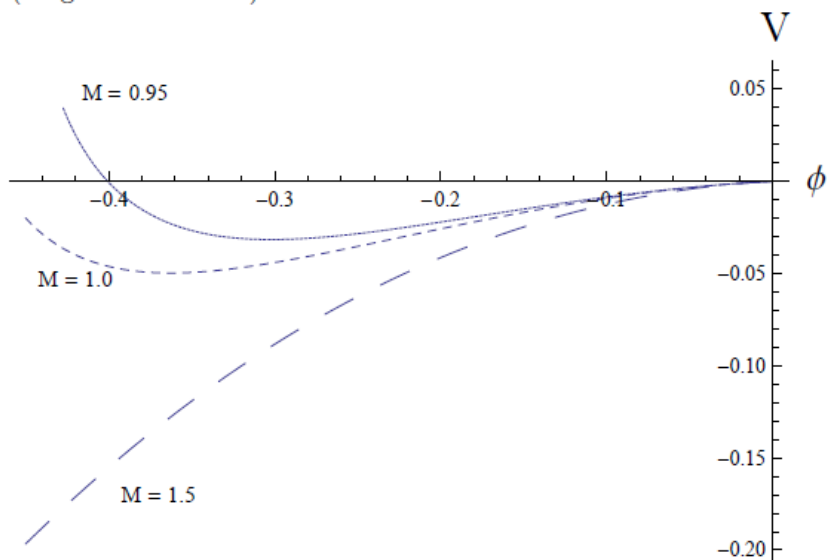


FIGURE 6. The variation of the Sagdeev potential $V(\phi)$ with position ϕ for the different values of M , the soliton velocity. $M = 0.95$ (solid curve), $M = 1.0$ (dotted curve) and $M = 1.5$ (long-dashed curve), where $\delta = 0.3$, $q = 1.2$, $\sigma = 0.036$, $\gamma = 0.52$, $\mu = 0.46$.

IV. PSEUDO-POTENTIAL APPROACH AND DISCUSSIONS

To study time-dependent solitary structure, we consider that all the dependent variables depend only on a single variable ξ , which follows the following relation.

$$\xi = X - MT, \quad (19)$$

where ξ is normalized by λ_d and M is the Mach number defined by the ratio of soliton velocity and C_d .

Now using equation (19) in equation (6) - (8), we get the following set of equations:

$$-M \frac{dN}{d\xi} + \frac{d(NU)}{d\xi} = 0, \quad (20)$$

$$-M \frac{dU}{d\xi} - \frac{dU}{d\xi} = \frac{d\Phi}{d\xi}, \quad (21)$$

$$\frac{d^2\phi}{d\xi^2} = \frac{1}{\mu} [\gamma \{1 + (q-1)\sigma\phi\}^{(1+q)/2(q-1)} - \left\{1 - \phi - \frac{4}{3\sqrt{\pi}}(1-\delta)(-\phi)^{3/2} + \frac{1}{2}\phi^2\right\} + \mu N], \quad (22)$$

The boundary conditions are: $\phi, U \rightarrow 0$, and $N \rightarrow 1$ as $|\xi| \rightarrow \infty$.

From equation (20), we get

$$N = \frac{M}{M - U}, \quad (23)$$

From equation (21) we get

$$\phi = -MU + \frac{U^2}{2}, \quad (24)$$

Now using equations (23)-(24) in equation (22) we get

$$\frac{d^2\phi}{d\xi^2} = -\frac{\partial V(\phi)}{\partial \phi}, \quad (25)$$

where

$$V(\phi) = \frac{2\gamma}{\sigma\mu(3q-1)} \left[1 - \{1 + (q-1)\sigma\phi\}^{\frac{3q-1}{2(q-1)}} \right] + M^2 \left[1 - \left(1 + \frac{2\phi}{M^2} \right)^{1/2} \right] + \frac{1}{\mu} \left[\phi - \frac{\phi^2}{2} + \frac{8}{15\sqrt{\pi}}(1-\delta)(-\phi)^{5/2} + \frac{1}{6}\phi^3 \right] \quad (26)$$

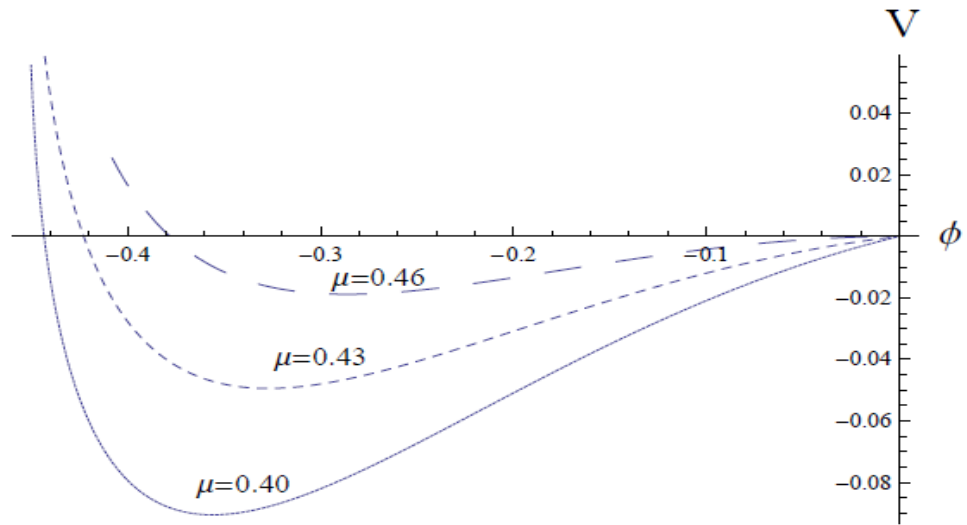


FIGURE 7. The variation of the Sagdeev potential $V(\phi)$ with position ϕ for the different values of μ , i.e., $\mu = 0.40$ (solid curve), $\mu = 0.43$ (dotted curve) and $\mu = 0.46$ (long-dashed curve), where $M = 0.95$, $\delta = 0.3$, $q = 1.2$, $\sigma = 0.036$, $\gamma = 0.52$.

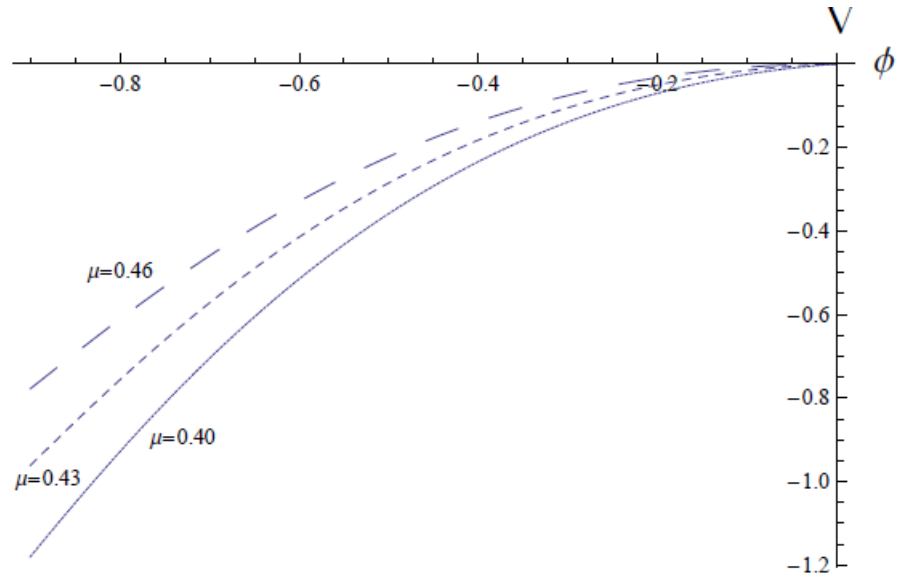


FIGURE 8. The variation of the Sagdeev potential $V(\phi)$ with position ϕ for the different values of μ , i.e., $\mu = 0.40$ (solid curve), $\mu = 0.43$ (dotted curve) and $\mu = 0.46$ (long-dashed curve), where $M = 1.5$, $\delta = 0.3$, $q = 1.2$, $\sigma = 0.036$, $\gamma = 0.52$.

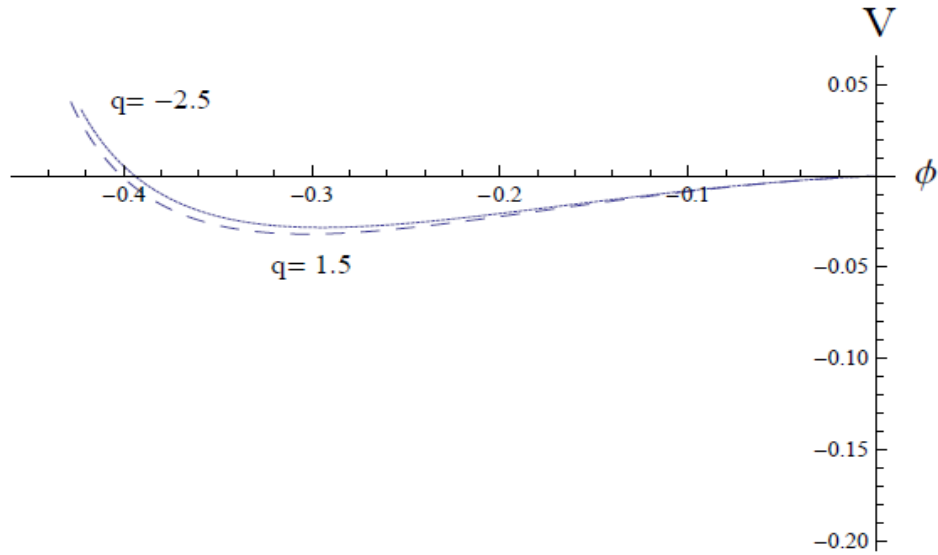


FIGURE 9. The variation of amplitude Φ_m with non-extensive parameter $q = -2.5$ (solid curve) and $q = 1.5$ (dotted curve) for $M = 0.95$.

Multiplying both sides of equation (26) by $2 \frac{d\phi}{d\xi}$ and integrating w. r. to ξ with the boundary conditions $|\xi| \rightarrow \infty, V \rightarrow 0$ and $\frac{d\phi}{d\xi} \rightarrow 0$, we get

$$V(\phi) + \frac{1}{2} \left(\frac{d\phi}{d\xi} \right)^2 = 0. \tag{27}$$

Equation (27) can be considered as a motion of a particle (whose pseudo-position is ϕ at pseudo-time ξ) with pseudo-velocity $\frac{d\phi}{d\xi}$ in a pseudo-potential well $V(\phi)$. That is why Sagdeev’s potential is called pseudo-potential. Hence the conditions for the existence of solitary wave solutions are:

(i) It is clear from equation (27) that $V(\phi) = dV(\phi)/d\phi = 0$ at $\phi = 0$. Therefore, the solitary wave solution of equation (27) only exist if $d^2V/d\phi^2 < 0$ at $\phi = 0$.

(ii) There exists a non-zero ϕ_m , the maximum (or minimum) value of ϕ where $V(\phi_m) = 0$, ϕ_m is the amplitude of the solitary wave. If ϕ_m is positive then the solitary wave is called compressive solitary wave, and if ϕ_m is negative then the solitary wave is called rarefactive solitary wave.

(iii) $d^3V/d\phi^3 > (<)0$ for solitary waves with $\phi > (<)0$. The nature of these solitary waves, whose amplitude tends to zero as the Mach number M tends to its critical value, can be found from the cubic term. If the cubic term is negative, there is a potential well in the negative side and if the cubic

term is positive, there is potential well in the positive side. In this numerical analysis indicates that the cubic term is always negative, i. e., solitary waves with $\phi < 0$ can only exist. In this model, solitary waves with $\phi > 0$ cannot exist.

Figures 6-9 display the results of investigations when Sagdeev's pseudo-potential technique is applied.

Figure 6 shows the variation of Sagdeev potential $V(\phi)$ as a function of position ϕ for different values of Mach number (M), the soliton velocity. The solid curve, the dotted curve and long-dashed curve are for $M = 0.95$, $M = 1.0$ and $M = 1.5$, respectively. It is clearly seen that there is an effect of Mach number on pseudo-potential. It is found that the positive and negative potentials are exist when soliton velocity (Mach number) is lower but only negative potential exists when the Mach number is higher ($M = 1.5$). If the Mach number $M \leq 1$ then potential shows negative initially then it changes to positive. But for higher value of Mach number $M = 1.5$, the potential is always negative and decreases.

Figure 7 displays the variation of potential $V(\phi)$ as a function of position ϕ with different values of μ for lower value of Mach number ($M = 0.95$). The solid curve, the dotted curve and long-dashed curve are for $\mu = 0.40$, $\mu = 0.43$ and $\mu = 0.46$, respectively. Potential changes with the change of μ . The amplitude of the solitary wave decreases with the increasing of μ . It indicates that when the number of dust grains in the plasma increases then the solitary wave's amplitude decreases. For a certain value of ϕ the potential changes from negative to positive.

Figure 8 shows the variation of potential $V(\phi)$ as a function of position ϕ with different values of μ for higher value of Mach number ($M = 1.5$). The solid curve, the dotted curve and long-dashed curve are for $\mu = 0.40$, $\mu = 0.43$ and $\mu = 0.46$, respectively. It is found that the potential is always negative and decreases for higher value of $M = 1.5$. In case of higher Mach number, the change of dust grains number is not much effective for the change of potential. For the lower value of Mach number the solitary wave has positive potential as well as negative potential but when the Mach number is higher than it has only negative potential.

Figure 9 shows the variation of the amplitude ϕ_m with the different values of electron non-extensivity. It would be concluded that the higher (lower) value of non-extensive parameter q the solitary wave amplitude is significantly increased (decreased). This may be due to the electron non-extensivity. Since electron is very lighter than ion, it avails the energy swiftly comparing ion and dust. As a result the potential growing in the solitary wave is clearly visible. Thereafter high energy trails [17–19] are formed and it varies due to different non-extensive parameter q .

V. CONCLUSION

In this work, we have addressed the problem of 1D DA Solitary waves in a dusty plasma with nonextensive electrons and vortex-like distributed ions. Here, modified KdV equation is derived by

using the standard reductive perturbation technique and a detailed numerical analysis of amplitude, width and phase velocity of the DA wave is performed. For the numerical analysis of arbitrary amplitude of DA solitary waves, Sagdeev's pseudo-potential approach is also incorporated in the present work. It is found that by increasing the number of trapped ions the potential of the solitary wave increases, but by increasing the nonextensive parameter q the potential of the solitary wave also increases. We observed that phase velocity and the width of the solitary waves increase with μ and decrease with the nonextensive parameter q . Also we have found that the amplitude of the solitary wave increases with both δ and q .

We found from the Sagdeev's pseudo-potential analysis that the positive and negative potentials are exist in the plasma system when the soliton velocity is less but only negative potential is noticed for the higher soliton velocity.

It is stressed that the increase of the value of non-extensive parameter q the solitary wave amplitude is significantly increased. The wave amplitude is significantly changed due to the presence of high energetic non-Maxwellian nonextensive electron. This is due to the anisotropy of the temperature and long range interactions caused by the coupling between plasmas and external fields. The results of the present investigation of DA solitary waves in presence of nonextensive electrons and trapped ions can also be very useful for understanding the plasma of Earth's mesosphere, Noctilucent Clouds, Polar Mesosphere summer Echoes, etc. where high energy tails [18, 19, 21] can be visible.

Further studying the effect of nonextensive electrons on Shock structures is beyond the scope of this paper. The magnetic field effect can also be further investigated.

-
1. E. I. El-Awady and M. Djebli, *Can. J. Phys.* **90**, 675 (2012).
 2. P. K. Shukla and A. A. Mamun, *Introduction to Dusty Plasma Physics*, IoP Publishing Ltd., Bristol (2002).
 3. V. E. Fortov, A. G. Khrapak, S. A. Khrapak, V. I. Molotkov, and O. F. Petrov, *Phys. Usp.* **47**, (2004).
 4. V. E. Fortov, A. Ivlev, S. Khrapak, A. Khrapak, and G. Morfill, *Phys. Rep.* **421**, 1 (2005).
 5. O. Ishihara, *J. Phys. D* **40**, R121 (2007).
 6. P. K. Shukla and B. Eliasson, *Rev. Mod. Phys.* **81**, 25 (2009).
 7. P. K. Shukla and B. Eliasson, *Phys. Rev. E* **86**, 046402 (2012).
 8. N. N. Rao, P. K. Shukla and M. Y. Yu, *Planet. Space Sci.* **38**, 543 (1990).
 9. A. Barkan, R. L. Merlino, and N. D'Angelo, *Phys. Plasmas*. **2**, 3563 (1995).
 10. A. A. Mamun, *J. Plasma Phys.* **59**, 575 (1998).
 11. M. Emamuddin, S. Yasmin, and A. A. Mamun, *Phys. Plasmas* **20**, 043705 (2013).
 12. M. Asaduzzaman and A. A. Mamun, *Astrophys. Space Sci.* **341**, 535 (2012).
 13. A. A. Mamun, *Phys. Lett. A* **372**, 884 (2008).
 14. M. Asaduzzaman and A. A. Mamun, *J. Plasma Phys.* **78**, 125 (2012).
 15. T. E. Sheridan, V. Nosenko, and J. Goree, *Phys. Plasmas* **15**, 073703 (2008).
 16. P. Bandyopadhyay, G. Prasad, A. Sen, and P. K. Kaw, *Phys. Rev. Lett.* **101**, 065006 (2008).
 17. C. Tsallis, *J. Stat. Phys.* **52**, 479 (1988).

18. F. Nobre and C. Tsallis, *Physica A* **213**, 337 (1995)
19. M. Sakagami and A. Taruya, *Contin. Mech. Thermodyn.* **16**, 279 (2004).
20. A. R. Plastino and A. Plastino, *Phys. Lett.* **174**, 384 (1993).
21. G. Gervino, A. Lavagno and D. Pigato, *Central Eur. J. Phys.* **10**, 594 (2012).
22. A. Vergou, *J. Phys. Conf. Ser.* **171**, 012035 (2009).
23. M. Tribeche and A. Merriche, *Phys. Plasmas* **18**, 034502 (2011).
24. P. Eslami, M.Mottaghizadeh and H.R. Pakzad, *Can. J. Phys.* **90**, 16 (2012)
25. S. Yasmin, M. Asaduzzaman and A.A. Mamun, *Astrophys. Space Sci.* **343**, 245 (2013).
26. M. Tribeche and L. Djebarni, *Phys. Plasmas* **17**, 124502 (2010).
27. H. R. Pakzad, *Can. J. Phys.* **89**, 1073 (2011).
28. K. Roy, P. Chatterjee, S. S. Kausik, and C. S. Wong, *Astrophys. Space Sci.* **350**, 599 (2014)
29. P. K. Shukla, *Phys. Plasmas* **8**, 1791 (2001).
30. M. Emamuddin, S. Yasmin, M. Asaduzzaman, and A. A. Mamun, *Phys. Plasmas* **20**, 083708 (2013).
31. J. X. Ma and J. Liu, *Phys. Plasmas* **4**, 253 (1997).
32. M. R. Amin, Sanjit K. Paul, Gurudas Mandal and A. A. Mamun, *J. Plasmas Phys.* **76**, 477 (2010).
33. H. Alinejad, *Astrophys. and Space Sci.* **325**, 209 (2009).
34. H. Washimi and T. Sarma, *Phys. Rev. Lett.* **17**, 996 (1966).
35. S G Tagare, *Phys. Plasma* **4**, 3167 (1997)
36. B. Xie, K He and Z Huang, *Phys. Lett. A* **247**, 403(1998)
37. B. Xie, K He and Z Huang, *Phys. Plasma* **6**, 3808(1999)
38. S I Popel, S I Kopnin, I N Kosarev and M Y Yu, *Advances in Space res.* **37**, 414 (2006).
39. W. S. Duan, *Phys. Lett. A* **317**, 275 (2003).
40. A. A. Mamun, R A Cairns and P. K. Shukla, *Phys. Plasmas* **3**, 2610 (1996).
41. Jingyu Gong and Jiulin Du, *Phys. Plasmas* **19**, 023704 (2012).
42. H. Schamel, *J. Plasma Phys.* **14**, 905 (1972).
43. H. Schamel, *J. Plasma Phys.* **9**, 377 (1973).